euspen's 22nd International Conference & Exhibition, Geneva, CH, May/June 2022
www.euspen.eu

Rectilinear translation four-bar flexure mechanism based on four Remote Center Compliance pivots

Loïc Tissot-Daguette[1], Hubert Schneegans[1], Quentin Gubler[1], Charles Baur[1] and Simon Henein[1]

[1]*Instant-Lab, EPFL, Switzerland*

loic.tissot-daguette@epfl.ch

Abstract
This paper presents a novel planar four-bar linkage compliant mechanism (called *4-RCC*) based on four flexure-based Remote Center of Compliance (RCC) pivots. With particular configurations and dimensions, the beam shortening of the RCC pivots can compensate the parasitic shift of the four-bar linkage over its range of motion, thereby creating a rectilinear translation mechanism. Moreover, to decrease the stiffness in the direction of the desired translation, while keeping the same magnitude of the transversal stiffnesses, a fixed-guided buckled beam with constant negative stiffness is added in parallel. This stiffness compensation greatly decreases the force to actuate the stage. This paper derives the analytical conditions required to compensate both the parasitic shift and the stiffness of the *4-RCC* mechanism. A mesoscale mockup model is designed, aiming for a millimeter-scale stroke, a compensated parasitic shift and a near-zero stiffness. A finite element model (FEM) validates the mechanism design and the analytical model. Simulation results show that the design leads to a parasitic shift below 65.6 nm over a displacement range of 8 mm, and the required actuation force is reduced by 95% when the buckled beam is added. Furthermore, the residual straightness error can be minimized by advantageously adjusting the preload of the buckled beam.

Flexures, Rectilinear mechanism, Zero-force, Negative stiffness, Beam buckling

1. Introduction

Compliant mechanisms offer several advantages, such as no friction, no backlash, no required lubrication and the possibility of monolithic manufacturing, allowing repeatable and accurate motions for rectilinear translation stages [1]. However, compliant mechanisms also present some drawbacks, such as a limited stroke relatively to its overall volume, an undesirable parasitic motion and an elastic restoring force.

Rectilinear compliant mechanisms are often based on exact or approximate straight-line motion linkages where the joints are replaced by flexures [2-4]. Another common approach is to compensate the parasitic motion of the rigid-body linkage kinematics with the parasitic shift of its flexural joints [5, 6].

In this paper, a novel planar compact four-bar mechanism using four RCC flexure pivots, called *4-RCC*, is presented. Its rectilinear translational motion is realized using the parasitic shift compensation approach. A buckled beam with negative stiffness, similarly to Ref. [7], is added to reduce the translational stiffness of the compliant mechanism. As the parasitic motion of flexure pivots is sensitive to external loads [8], the preload from the buckled beam must be considered in the design of the compliant mechanism.

The *4-RCC* mechanism is described, modeled and designed in Sects. 2, 3 and 4, respectively. The design and the modeling are validated in Sect. 5 using FEM simulation. Finally, the rectilinearity and the stiffness reduction are discussed in Sect. 6 and perspectives of this work are addressed in Sect. 7.

2. Mechanism description

The new rectilinear translation mechanism proposed in this paper is described in this section. Its kinematic architecture is based on a parallelogram linkage with four pivots R, S, T and U having the same angular stiffness K_α. If the pivots have no parasitic motion when rotated, the mechanism guides the output stage over a distance x with a parasitic shift $\Delta y_{\text{linkage}}$ (Fig. 1). Instead, using four RCC pivots with an inherent parasitic motion Δy_{RCC} in the bisector direction of their beams (Fig. 2), the parasitic shift of the parallelogram linkage can be compensated. This leads to the *4-RCC* flexure-based kinematics shown in Fig. 3, which, with specific dimensions, provides a rectilinear translation of the stage.

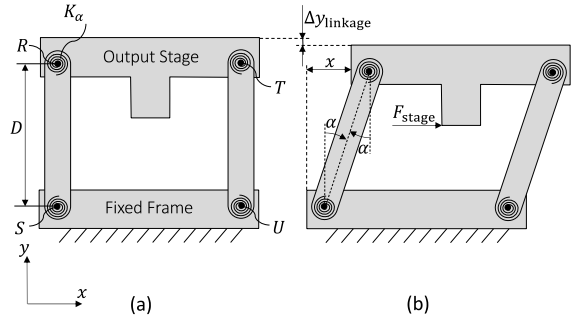

Figure 1. Parasitic shift of planar four-bar linkage. The output stage is (a) in neutral position and (b) in deformed position.

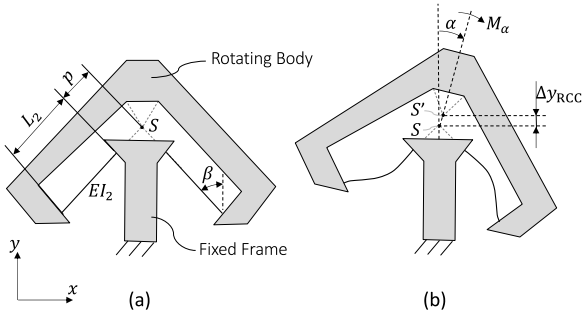

Figure 2. Parasitic shift SS' of a RCC pivot. The pivot is (a) in neutral position and (b) deformed.

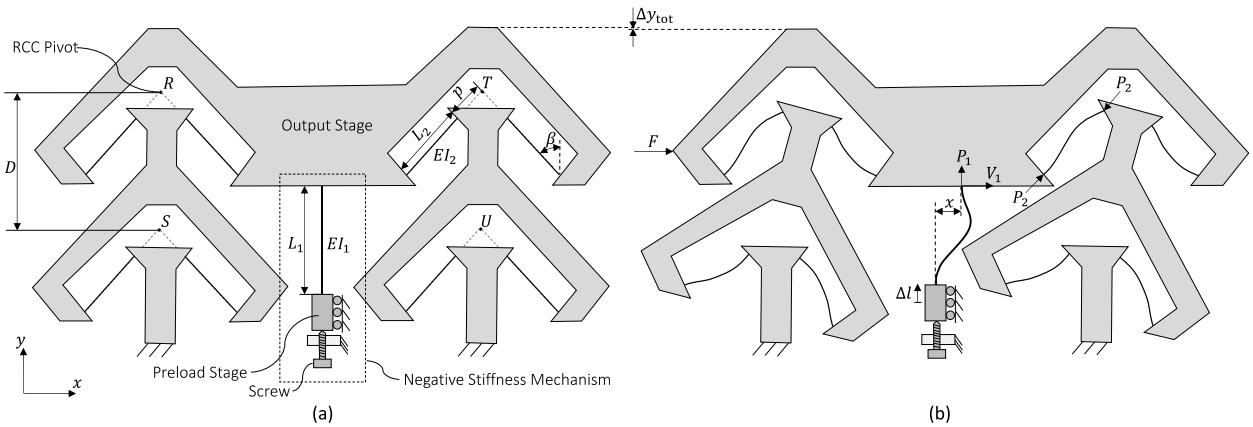

Figure 3. *4-RCC* rectilinear translation stage represented (a) as-fabricated and (b) deformed. Note that P_1, V_1 and P_2 are internal forces.

In order to decrease the actuation force F, a negative stiffness mechanism is added in parallel, which compensates the positive stiffness of the compliant stage (Fig. 3). The negative stiffness is provided by the force V_1 along the x-axis of a fixed-guided buckled beam. The end-shortening of the buckled beam is controlled by the displacement Δl of a preload stage (schematically actuated by a screw in Fig. 3). Depending on the dimensions of the buckled beam, it is possible to compensate the primary stiffness, leading to a near-zero-force mechanism.

As the buckling load P_1 applies a compressive force P_2 in each RCC pivot beams, it involves a higher parasitic shift Δy_{RCC} of the RCC pivots than if they were not loaded [8].

3. Analytical model

This section introduces the theoretical model used to design a *4-RCC* rectilinear translation stage with stiffness compensation. For the calculations, we assume that the beams of the RCC pivots and the buckled beam are slender and initially straight. We consider that all the pivots have the same dimensions and their centers of rotation (i.e., points R, S, T and U) form a rectangle when the stage is at neutral position and a parallelogram when deformed. We assume that the beams of all the RCC pivots have the same compressive force P_2, even when the compliant stage is deformed. The small deformation hypothesis is assumed for all flexure elements, i.e., the RCC pivot angular stroke α is small and the end-shortening of the buckled beam Δl is small compared to its length L_1. The flexural rigidities of the buckled beam and the RCC pivot beams, respectively EI_1 and EI_2, are considered constant along the beam length. The out-of-plane thickness (i.e., along the z-axis, perpendicular to the xy-plane) of the mechanism is large enough to constrain the output stage motions in the xy-plane. Gravity and dynamics are neglected in this model.

3.1. Parasitic motion compensation

The parasitic translation of the *4-RCC* output stage is equal to the difference between the four-bar linkage parasitic shift and two times the parasitic shift of one RCC pivot (see Figs. 1-3):

$$\Delta y_{\mathrm{tot}} = \Delta y_{\mathrm{linkage}} - 2\Delta y_{\mathrm{RCC}} \tag{1}$$

Considering small angle deformations, the parasitic shift of the four-bar linkage is approximated by its 2nd degree Taylor series expansion around $\alpha = 0$:

$$\Delta y_{\mathrm{linkage}} = D(1-\cos(\alpha)) \cong \frac{D\alpha^2}{2} \tag{2}$$

where D is the nominal height of the parallelogram $RSTU$. The RCC pivot parasitic motion can be computed geometrically using the end-shortening formula of a fixed-pinned precompressed beam [9]. Considering the beam length L_2, the ratio $\bar{p} = p/L_2$ and the angle β (see Fig. 3), it gives:

$$\Delta y_{\mathrm{RCC}} = 2\cos(\beta)\, H(kl) L_2 \alpha^2 \tag{3}$$

where:

$$\begin{aligned} H(kl) = \frac{kl}{8}[&\bar{A}^2(6kl - 8\sin(kl) + \sin(2kl)) \\ &+2\bar{A}\bar{B}(\cos(2kl) - 4\cos(kl) + 3) \\ &+\bar{B}^2(2kl - \sin(2kl))] + \frac{\bar{p}}{2} \end{aligned} \tag{4}$$

$$\bar{A} = \frac{\cos(kl) - 1 - kl\,\bar{p}\sin(kl)}{kl\big(kl\sin(kl) + 2(\cos(kl) - 1)\big)} \tag{5}$$

$$\bar{B} = \frac{kl - \sin(kl) - kl\,\bar{p}(\cos(kl) - 1)}{kl\big(kl\sin(kl) + 2(\cos(kl) - 1)\big)} \tag{6}$$

In our case, the compression parameter is $k = \sqrt{P_2/EI_2}$ and the beam length is $l = L_2$, thus:

$$kl = \sqrt{\frac{P_2}{EI_2}} L_2 \tag{7}$$

From Fig. 3b, the forces P_1 and P_2 have the following relationship:

$$P_2 = \frac{P_1}{4\cos(\beta)} \tag{8}$$

Assuming that the buckled beam is in the constant negative stiffness state, the force P_1 is equal to the second buckling load of a fixed-guided beam [7]:

$$P_1 = \frac{4\pi^2 EI_1}{L_1^2} \tag{9}$$

Note that P_1 is considered constant regardless of the preloading displacement Δl. However, to stay in the negative stiffness state the following constraint must be respected [7]:

$$\Delta l \geq \Delta l_{\min} = \frac{3}{4}\frac{x_{\max}^2}{L_1} \tag{10}$$

where $x_{\max}$ is the maximum stroke of the output stage in one direction. From Eqs. (7)-(9), kl becomes a function of the mechanism dimensions:

$$kl = \pi \sqrt{\frac{1}{\cos(\beta)} \frac{L_2}{L_1}} \sqrt{\frac{I_1}{I_2}} \tag{11}$$

The parasitic motion compensation is obtained if $\Delta y_{\text{tot}} = 0$, therefore from Eqs. (1)-(3), it gives the constraint condition:

$$\frac{D}{L_2} = 8 \cos(\beta)\, H(kl) \tag{12}$$

3.2. Primary stiffness compensation

The primary stiffness of the *4-RCC* output stage is the sum of the positive stiffness of the compliant four-bar linkage, and the negative stiffness of the buckled beam.

$$K_{x,\text{tot}} = \frac{F}{x} = K_{x,\text{pos}} + K_{x,\text{neg}} \tag{13}$$

For small displacement of the output stage, Ref. [1] gives the relationship between the stage linear stiffness and the hinge angular stiffness:

$$K_{x,\text{pos}} = \frac{F_{\text{stage}}}{x} = \frac{4K_\alpha}{D^2} \tag{14}$$

where the angular stiffness of a RCC pivot is [1]:

$$K_\alpha = \frac{M_\alpha}{\alpha} = 8 \frac{EI_2}{L_2} (1 + 3\bar{p} + 3\bar{p}^2) \tag{15}$$

According to Ref. [7], the negative stiffness of the buckled beam is equal to:

$$K_{x,\text{neg}} = -\frac{V_1}{x} = -\frac{4\pi^2 E I_1}{L_1^3} \tag{16}$$

From Eqs. (13)-(16), the stiffness compensation condition, i.e., $K_{x,\text{tot}} = 0$, requires that:

$$\frac{D}{L_1} = \frac{2\sqrt{2}}{\pi} \sqrt{\frac{L_1}{L_2} \frac{I_2}{I_1} (1 + 3\bar{p} + 3\bar{p}^2)} \tag{17}$$

4. Design of a zero-force *4-RCC*

In this section, a flexure-based mesoscale embodiment of the *4-RCC* aiming for a translation stroke of ±4 mm is designed (see Fig. 4 and table 1). The dimensions of the mechanism are derived from the analytical model presented in the previous section to achieve both parasitic shift and stiffness compensations. A large out-of-plane thickness $b = 20$ mm is selected to provide a high transversal stiffness. The half angle β is set to 45° to obtain an isotropic translational stiffness of the RCC pivots in the xy-plane. To make the mechanism monolithic and planar, the preload stage (Fig. 3) is replaced by a parallel leaf spring stage. The overall dimensions of the structure are 175 mm × 135 mm × 20 mm. The selected material of the flexure-based structure is the aluminum alloy EN AW 7075. It is chosen for its high yield stress on Young's modulus ratio σ_y/E (high flexibility) and for its low density on Young's modulus ratio ρ/E (low deformations due to gravity and high eigenfrequencies). The mechanism is meant to be manufactured by wire electrical discharge machining (EDM), enabling tight tolerances.

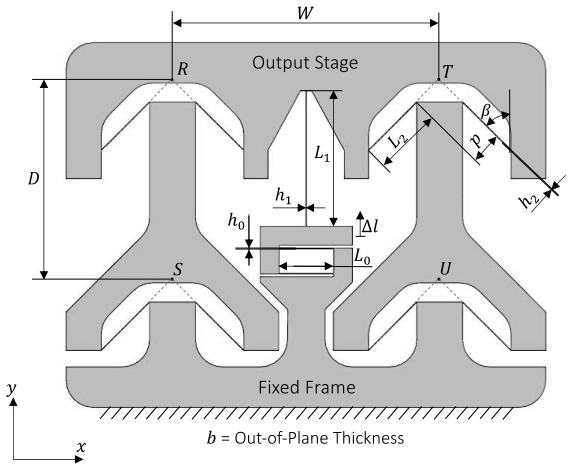

Figure 4. Mesoscale prototype of the *4-RCC* mechanism shown as-fabricated.

Table 1. Design parameters of the *4-RCC* mechanism.

Structure Part	Parameter	Value
Material (EN AW-7075)	E	72 GPa
	σ_y	480 MPa
	ρ	2810 kg/m³
Stage	$x_{\max}$	4 mm
	D	73.76 mm
	W	98.32 mm
	b	20 mm
RCC Pivot	h_2	150 µm
	L_2	25 mm
	p	12 mm
	β	45 deg
Buckled Beam	h_1	200 µm
	L_1	50 mm
Preload Stage	h_0	300 µm
	L_0	20 mm
	$\Delta l_{\min}$	0.375 mm

5. Simulation results

A finite element method (FEM) was carried out to characterize and validate the straightness and the stiffness reduction of the *4-RCC* designed in the previous section. A 2D plane stress stationary study was conducted on the commercial software COMSOL Multiphysics 5.6 with the "geometric nonlinearity" setting enabled. The displacement (x, y), the rotation around the z-axis θ_z and the actuation force F were evaluated on the output stage at a position $(W/2, -D/2)$ from point R (corresponding to the center of the parallelogram $RSTU$ when the stage is at rest). The simulation results are plotted in Fig. 5 for different end-shortenings Δl.

To characterize the rectilinearity of the output stage motion, we define the straightness error of the mechanism as the maximum deviation of $y(x)$ compared to the nominal offset $y(x = 0)$ (initial mechanism deformation due to the buckled beam load P_1), for the full motion range of ±4 mm. To evaluate the stiffness reduction, the *4-RCC* stage is simulated without the negative stiffness mechanism (i.e., the buckled beam is removed from the structure). Table 2 summarizes the major simulated characteristics of the stage for different end-shortenings Δl. We do not consider end-shortenings higher than $\Delta l = 2.5$ mm as the simulated maximum von Mises stress would exceed the material yield stress stated in table 1.

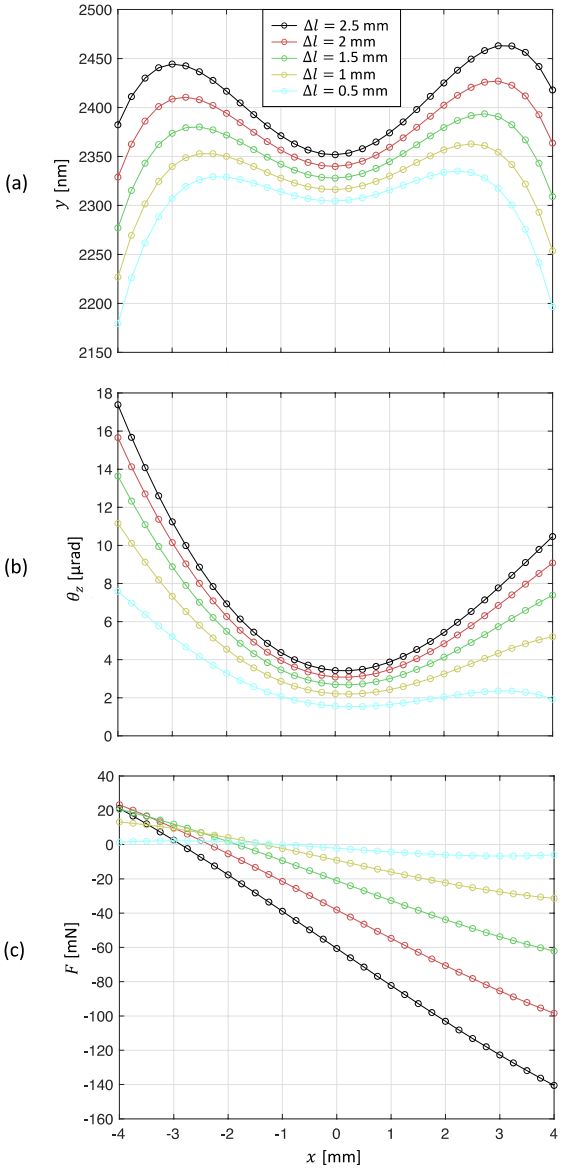

Figure 5. FEM results of the *4-RCC* rectilinear translation stage. (a) The lateral translation, (b) the parasitic rotation and (c) the actuation force are evaluated as a function of the primary motion, for different preloading displacements.

Table 2. Simulated characteristics of the *4-RCC* mechanism for a total stroke of ±4 mm.

Preloading	Straightness Error [nm]	Maximum Rotation [µrad]	Maximum Force [mN]	Maximum Stress [MPa]
Δl = 0.5 mm	125.2	7.6	6.7	185
Δl = 1 mm	89.4	11.2	31.4	260
Δl = 1.5 mm	65.6	13.6	62.1	318
Δl = 2 mm	87.1	15.7	98.4	368
Δl = 2.5 mm	111.2	17.4	140.5	411
No Buckled Beam	6163	0.13	1190	86

6. Discussions

Figure 5 shows that, as opposed to what has been predicted by the analytical model, the lateral displacement y, the parasitic rotation θ_z and the actuation force F of the *4-RCC* depend on the preloading displacement Δl. From table 2, it can be observed that adjusting the displacement Δl of the preload stage allows to advantageously minimize the straightness error. Indeed, the minimum straightness error is equal to 65.6 nm when selecting $\Delta l = 1.5$ mm, as the stage moves with the same amount of parasitic motion upwards and downwards for the considered stroke (see Fig. 5a). As the straightness error on total stroke ratio amounts only to 0.00082%, the *4-RCC* stage can be considered as an accurate rectilinear motion mechanism. The parasitic rotation θ_z, mainly caused by the reaction moment of the buckled beam applied on the moving stage, is considerably small with a maximum value of 13.6 µrad for the selected preload (i.e., $\Delta l = 1.5$ mm).

Adding the negative stiffness mechanism, the maximum actuation force F decreases from 1190 mN (no buckled beam) to 62.1 mN ($\Delta l = 1.5$ mm), leading to a stiffness reduction of 95%. Figure 5c shows an offset $F(x = 0)$, assumed to be primarily due to the parasitic motion of the parallel leaf spring stage. Note that the residual tangent stiffness of the mechanism (slope of the force-displacement curve in Fig. 5c) is negative. This behavior can be directly beneficial for bistable applications (e.g., force-limiting nanoprobing, microswitches, microvalves and nonvolatile memories).

7. Conclusion and future work

In this paper, a novel flexure-based four-bar planar rectilinear translation stage, called *4-RCC*, was designed. Analytical conditions were derived to design the mechanism with minimized parasitic shift and to compensate the primary stiffness of the output stage. FEM simulations validated the analytical model and the design: the mechanism shows a straightness error of 65.6 nm for a motion range of 8 mm and a stiffness reduction of 95% if a buckled beam with negative stiffness is added in parallel to the stage. Results show that the adjustment of the buckled beam end-shortening can beneficially minimize the parasitic shift of the output stage.

Future work includes the fabrication of a mesoscale prototype to experimentally validate the parasitic shift and the stiffness compensations of the *4-RCC*. Higher terms in the analytical model will be integrated to further optimize the mechanism dimensions. Depending on the application, the mechanism will be scaled up or down, and the dynamics and gravity effects will be investigated.

References

[1] Cosandier F, Henein S, Richard M and Rubbert L, 2017, *The Art of Flexure Mechanism Design*, EPFL Press, Lausanne

[2] Cosandier F, Eichenberger A, Baumann H, Jeckelmann B, Bonny M, Chatagny V and Clavel R, 2014, Development and integration of high straightness flexure guiding mechanisms dedicated to the METAS watt balance Mark II, *Metrologia,* **51**, S88-S95

[3] Hubbard N B, Wittwer J W, Kennedy J A, Wilcox D L and Howell L L, 2004, A novel fully compliant planar linear-motion mechanism, *ASME 2004 International Design Engineering Technical Conferences and Computers and Information in Engineering Conference*, Utah, USA

[4] Gräser P, Linß S, Harfensteller F, Torres M, Zentner L and Theska R, 2021, High-precision and large-stroke XY micropositioning stage based on serially arranged compliant mechanisms with flexure hinges, *Precision Engineering*, **72**, 469-479

[5] Pei X, Yu J, Zong G and Bi S, 2014, Design of compliant straight-line mechanisms using flexural joints, *Chinese Journal of Mechanical Engineering*, **27**, 146-153

[6] Zhao H, Bi S and Yu J, 2012, A novel compliant linear-motion mechanism based on parasitic motion compensation, *Mechanism and Machine Theory*, **50**, 15-28

[7] Vangbo M, 1998, An analytical analysis of a compressed bistable buckled beam, *Sensors and Actuators*, *A* **69**, 212-216

[8] Zhao H and Bi S, 2010, Accuracy characteristics of the generalized cross-spring pivot, *Mechanism and Machine Theory*, **45**, 1434-48

[9] Tissot-Daguette L, Smreczak M, Baur C and Henein S, 2021, Load cell with adjustable stiffness based on a preloaded T-shaped flexure pivot, *euspen's 21st International Conference & Exhibition, Copenhagen, DK*